Measurement of Higgs boson coupling properties to bosons with the ATLAS detector

M. BIGLIETTI - INFN ROMA 3

ON BEHALF OF THE ATLAS COLLABORATION

Introduction

- The Higgs boson has a rich set of properties that can be verified experimentally → powerful test of SM and constraint of BSM
- BSM can alter the Higgs boson production and decay
- measurements of the Higgs couplings with bosonic decay and their interpretation
  - Cross section and signal strength
  - Simplified Template Cross Section (STXS)
  - Couplings modifiers (k-framework)
  - Effective Fields Theories (EFT)

- Measurements based on an integrated luminosity of 139 fb^{-1}, collected from 2015 to 2018 at $\sqrt{s}$=13 TeV during LHC Run-2

Higgs to Vector Boson

H→WW : with large BR, has large backgrounds and limited mass resolution
H→γγ, H→ZZ→4l : low BR channels but cleaner with good mass resolution
not covered H→Zγ – *Phys. Lett. B 809 (2020)*

- all production mode considered

- each channel provides complementary information and probes different phase spaces

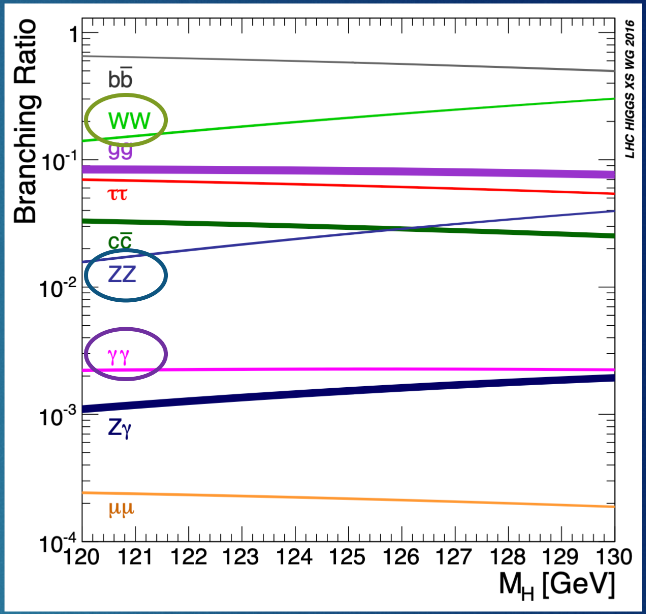

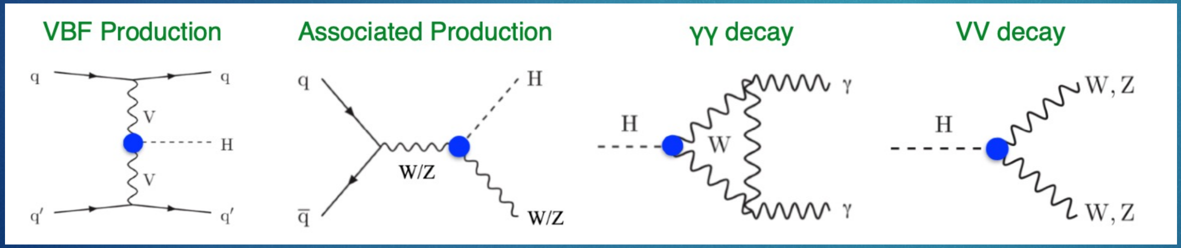

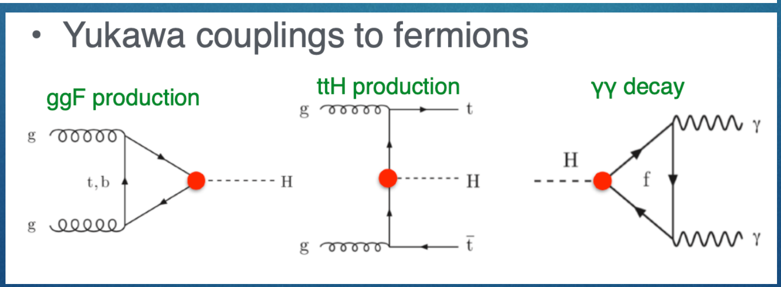

CERN-EP-2022-094
Eur. Phys. J. C 80 (2020) 957

H→γγ and H→ZZ→4l

- Higgs mass peak reconstructed on top of the relevant background, excellent mass resolution

- Background from sidebands
  - falling background composed by continuum γγ, γj, jj
  - non resonant ZZ, normalization constrained in different jet bins

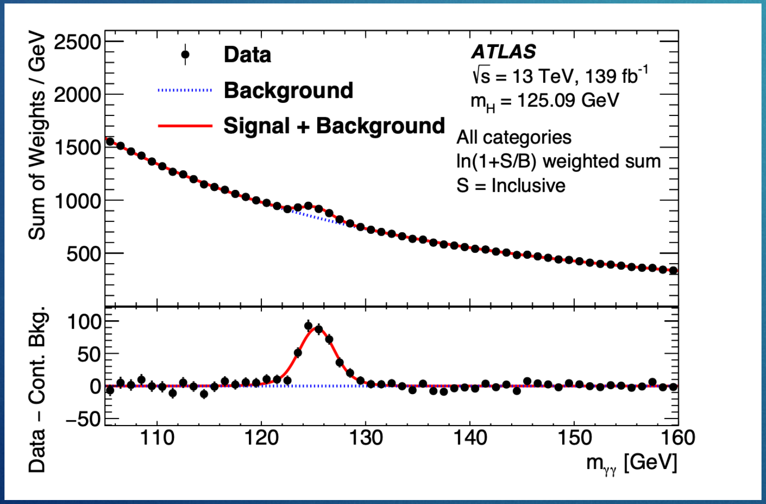

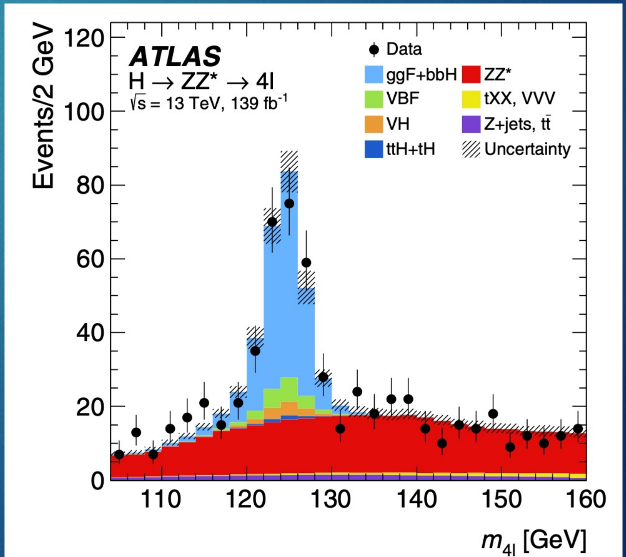

CERN-EP-2022-094
Eur. Phys. J. C 80 (2020) 957

$H \rightarrow \gamma\gamma$ and $H \rightarrow ZZ \rightarrow 4l$

- signal strength measured by simultaneously fitting the mass distributions of all analysis categories

$H \rightarrow \gamma\gamma$

$$\mu = 1.04^{+0.10}_{-0.09} = 1.04 \pm 0.06\,(\text{stat.})^{+0.06}_{-0.05}\,(\text{theory syst.})\,^{+0.05}_{-0.04}\,(\text{exp. syst.}).$$

$H \rightarrow 4l$

$$\mu = 1.01 \pm 0.08(\text{stat.}) \pm 0.04(\text{exp.}) \pm 0.05(\text{th.})$$

- main systematics uncertainties
  - experimental photon reconstruction and signal theory (QCD scale, Higgs BR)
  - lepton efficiency, luminosity, signal Parton shower

cross section measured for each production mode compatible with SM expectations

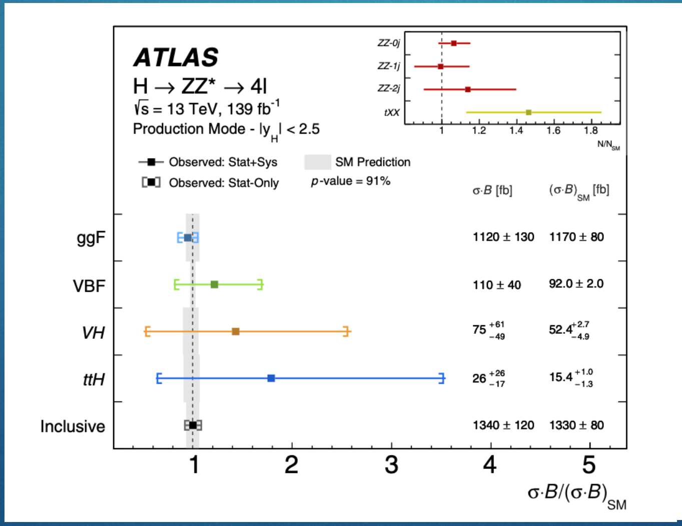

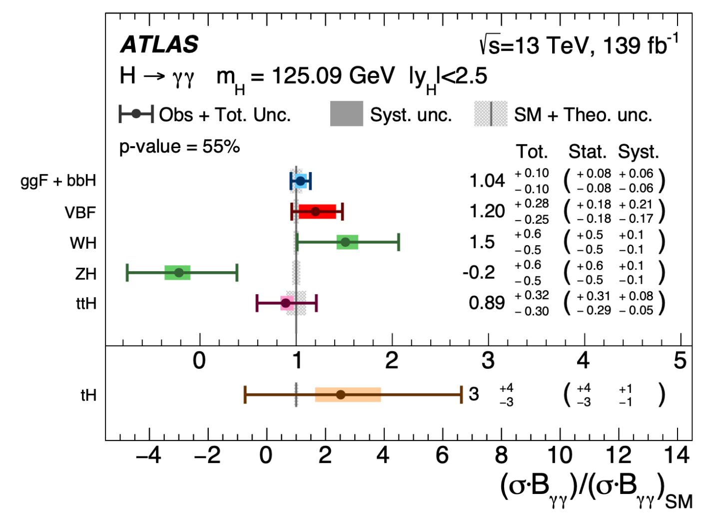

H→γγ - STXS

- 28 bins, optimized to avoid large uncertainties and correlation
- Categorization done with multiclass MVA to assign signal events in different STXS bins
  - improve the efficiency of event selection in production bins
  - Further binary classifiers to refine category selection and separate signal from background in each STXS bin

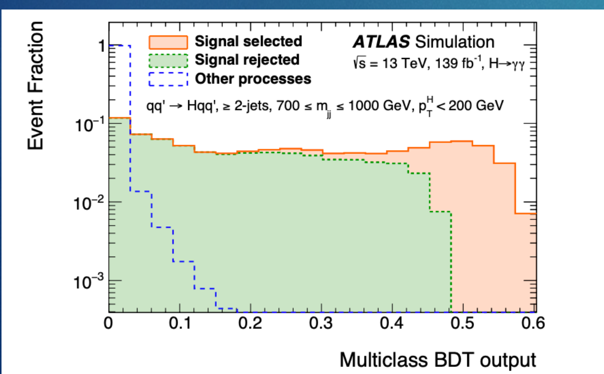

(b) $qq' \to Hqq'$, $\geq$ 2-jets, $700 < m_{jj} < 1000$ GeV, $p_T^H <$ 200 GeV

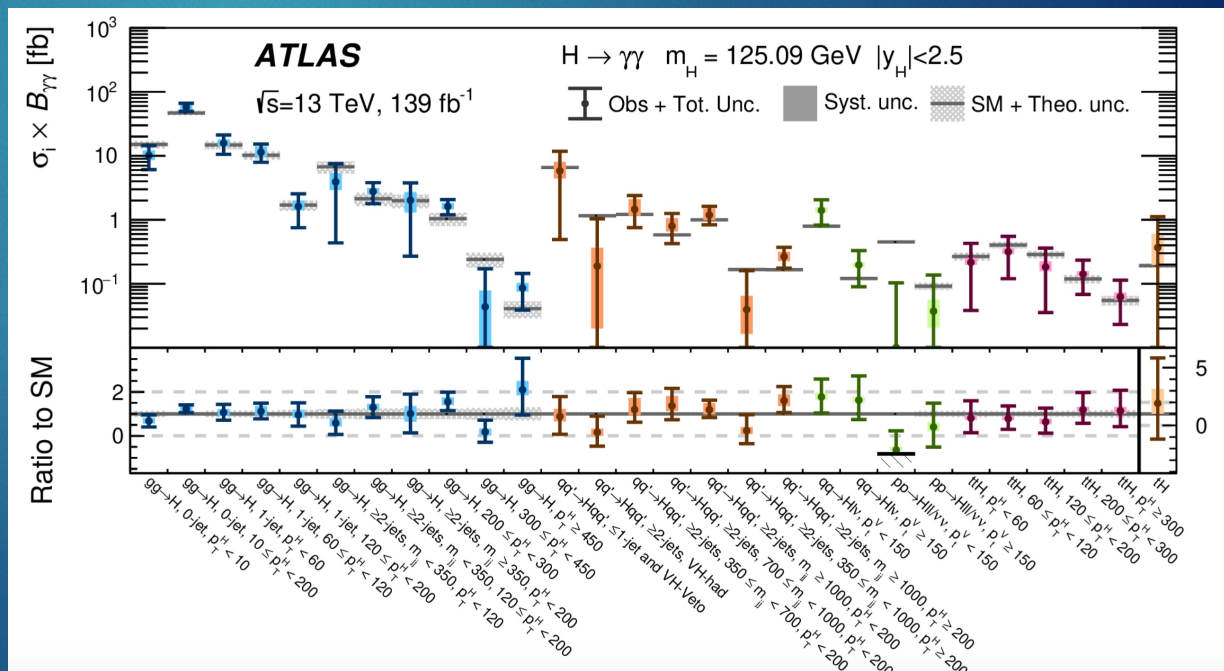

Eur. Phys. J. C 80 (2020) 957

H→ ZZ→4l – STXS

- 12 STXS bins measured/ 12 reconstructed categories
  - sidebands to estimate the top background in ttH category
- fit discriminants (NNs) in many categories to increase the sensitivity

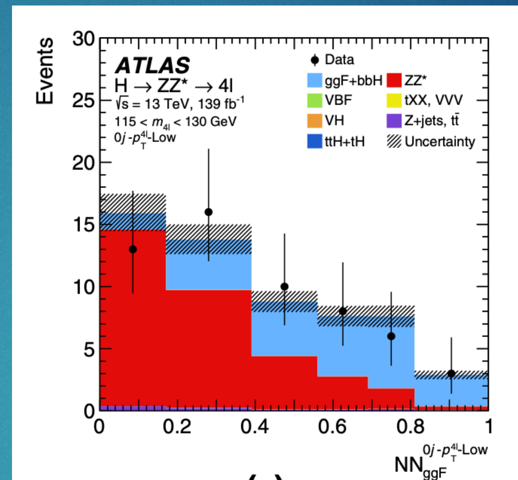

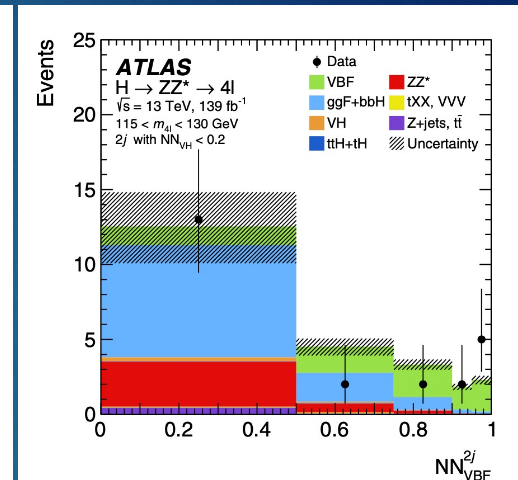

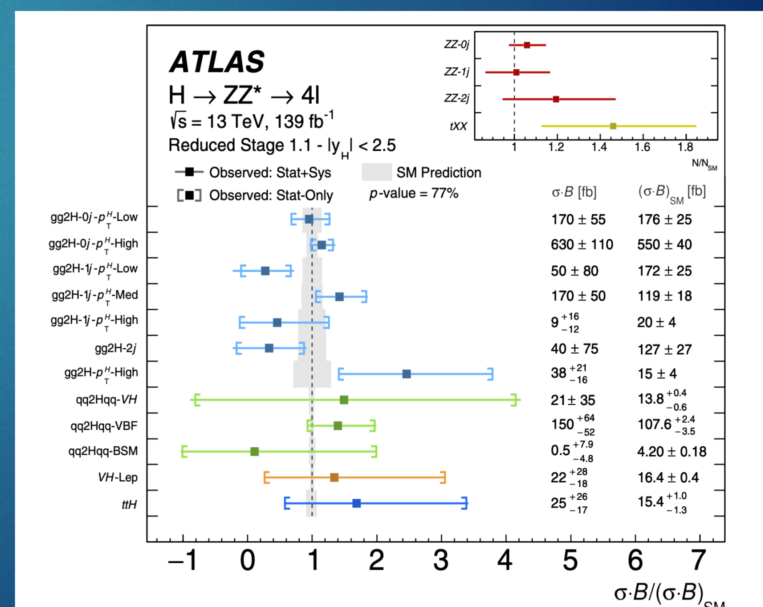

CERN-EP-2022-094
Eur. Phys. J. C 80 (2020) 957

Interpretation in the k-framework

- The Higgs cross-section in STXS regions written in terms of κ modifiers
- All other κ modifiers are fixed to their SM values

$$(\sigma_i \times B_f) = k_i^2 \sigma_i^{SM} \frac{k_f^2 \Gamma_f^{SM}}{k_H^2 \Gamma_H^{SM}}$$

measurement of κ_F and κ_V, probing the interactions of the Higgs sector with boson and fermions

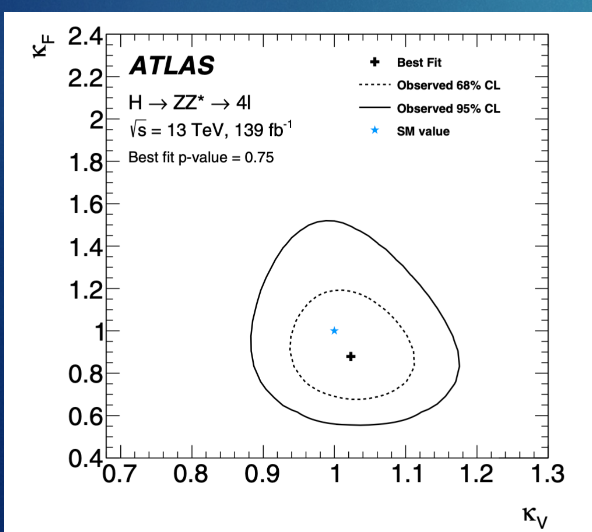

rates in gg→H and H→$\gamma\gamma$ described by effective modifieres κ_g and κ_γ

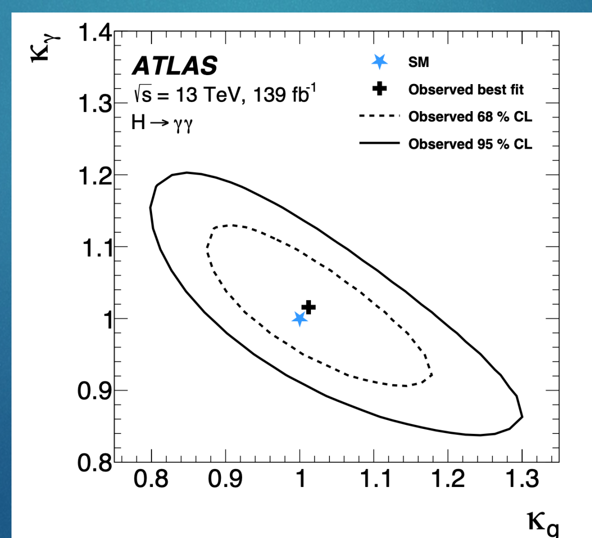

sign of κ_t from interference effects in tH, and in the H→$\gamma\gamma$ in resolved parametrisation

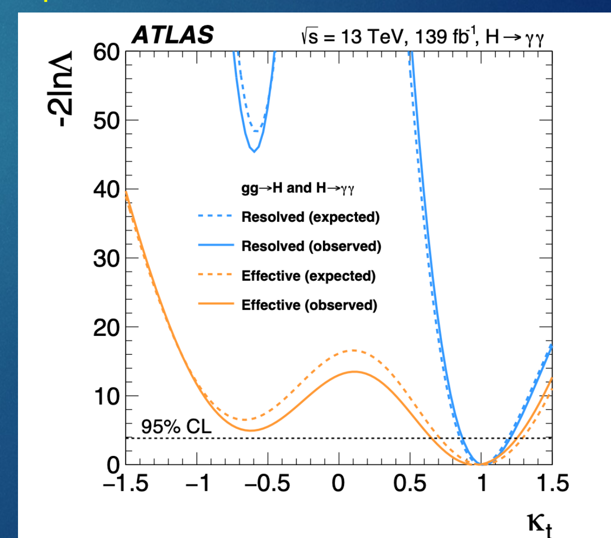

CERN-EP-2022-094
Eur. Phys. J. C 80 (2020) 957

H→γγ and H→ ZZ Interpretation in SMEFT

$$\mathcal{L}_{\mathrm{EFT}} = \mathcal{L}_{\mathrm{SM}} + \sum_i \frac{C_i^{(d)}}{\Lambda^{(d-4)}} \mathcal{O}_i^{(d)} \quad \text{for } d > 4.$$

- SMEFT Wilson coefficients determined through an interpretation of STXS results
  - in each production bin, cross sections, BRs and acceptance parametrised in terms of the Wilson coefficients
- Measurements of one SMEFT couplings assuming other are zero
- or meaurements of multiple coefficients by removing flat directions from PCA analysis of SMEFT information matrix
- linear/quadratic difference can be indicative of the

  impact of neglected higher-order terms in SMEFT

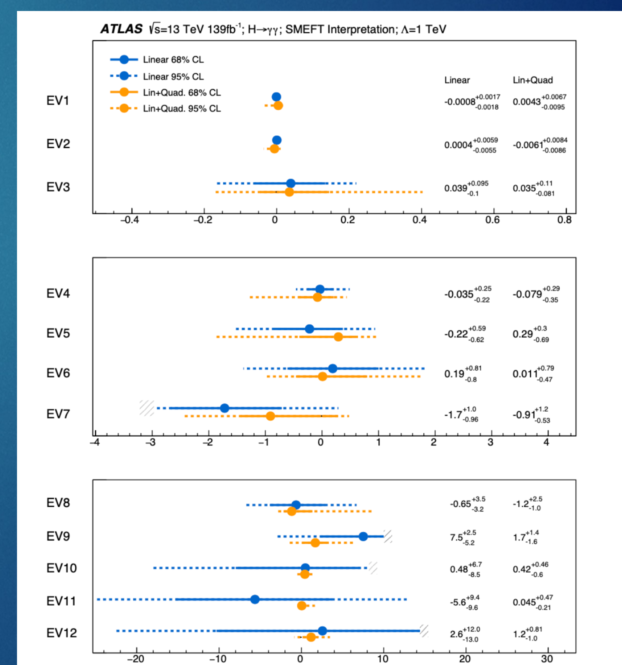

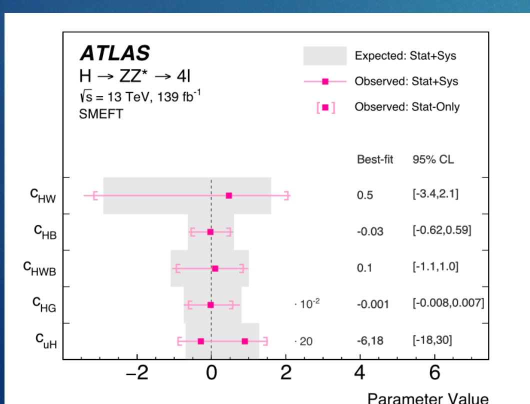

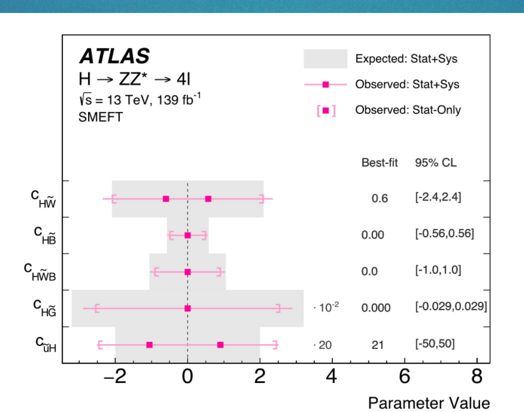

CERN-EP-2022-078

H→WW→lνlν (ggF and VBF production)

- Two charged isolated leptons of different flavour → less background from Z decays
- background composition depending on the number of jets in the final state → analysis performed separately in Njets=0,1,>=2 bins
  - Njets>=2 is split in ggF and VBF → 4 categories subsequently split in SR to increase the sensitivity
- control regions to normalize WW, top and Z+jets
- discriminating variables : di-lepton + ETmiss transverse mass m_T (ggF) and NN (VBF)

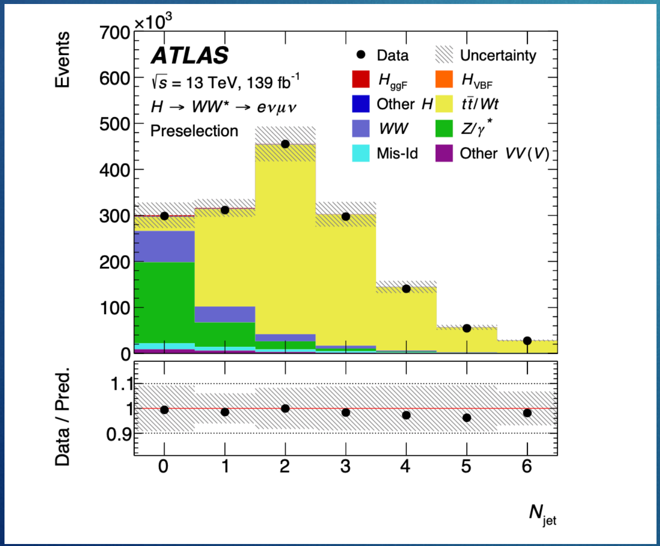

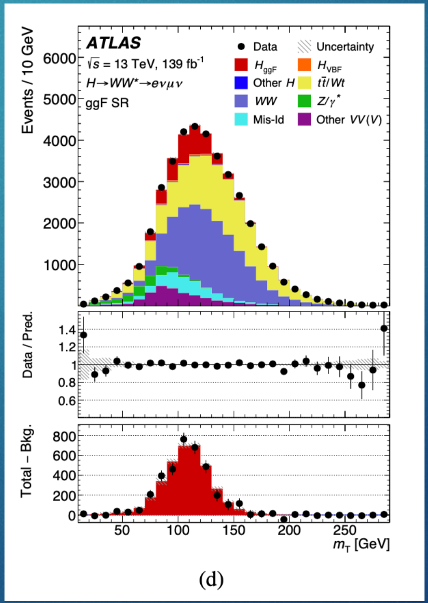

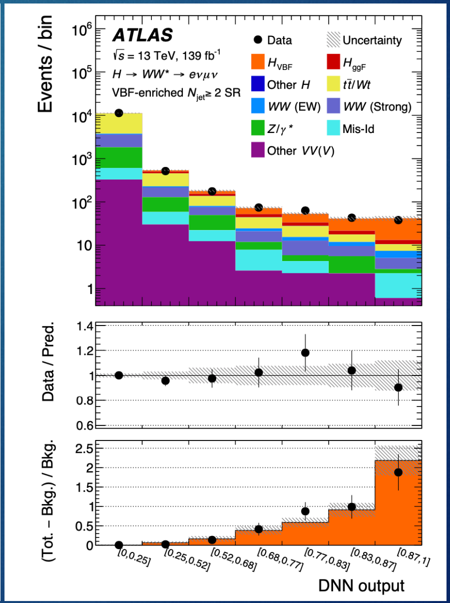

CERN-EP-2022-078

H→WW→lvlv (ggF and VBF production)

- Result from a simultaneous fit to all SRs
- inclusive measurements dominated by systematic uncertainties
  - ggF: exp and theory systematics comparable
  - VBF: signal theory uncertainties from additional jet modelling
- STXS : 6 bins for ggH and 5 for EW qqH production.
  - 12 reconstructed categories based on p_T^H and jet variables
  - Dedicated background CRs

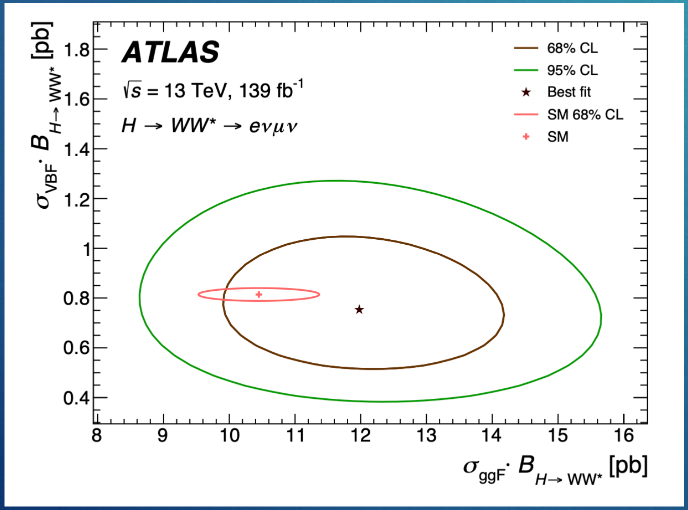

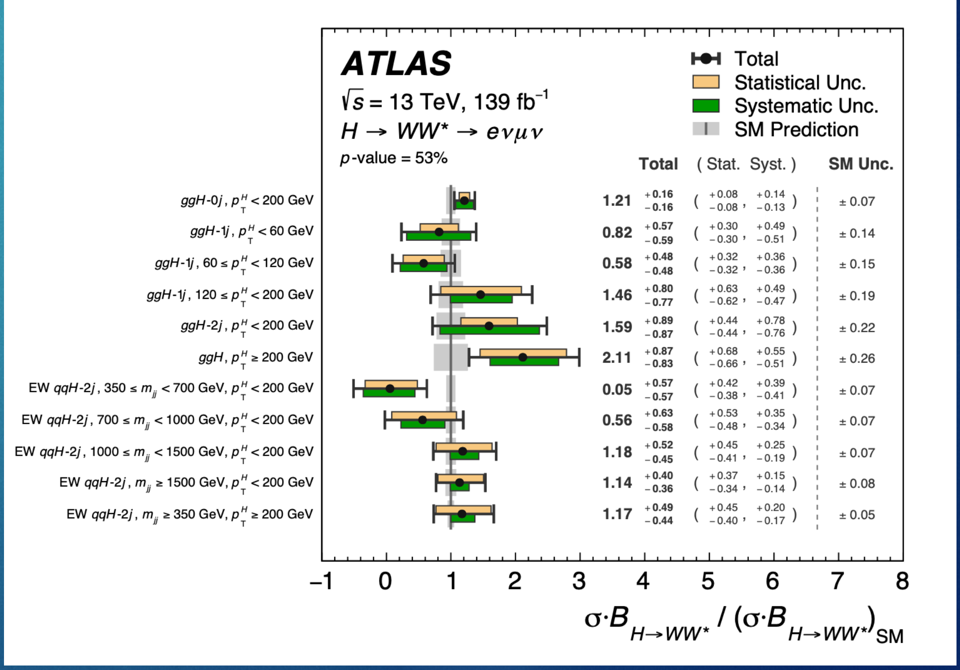

VH, H→WW

ATLAS-CONF-2022-067

- Direct access to couplings to weak bosons
- 2 (OS or SS), 3, or 4 charged isolated leptons

Channel	Normalised in the fit	Control Region	Data-driven
Opposite-sign 2ℓ	–	$t\bar{t}/Wt$, Z+jets, WW	W+γ, W+jets
Same-sign 2ℓ	$W(Z/\gamma^*)$	–	V+γ, V+jets
3ℓ	WWW	$W(Z/\gamma^*)$	Z+γ, Z+jets, $t\bar{t}/Wt$, WW+jets
4ℓ	–	ZZ	$W(Z/\gamma^*)$+jets, $t\bar{t}W/tZ$, Z+jets, $t\bar{t}/Wt$

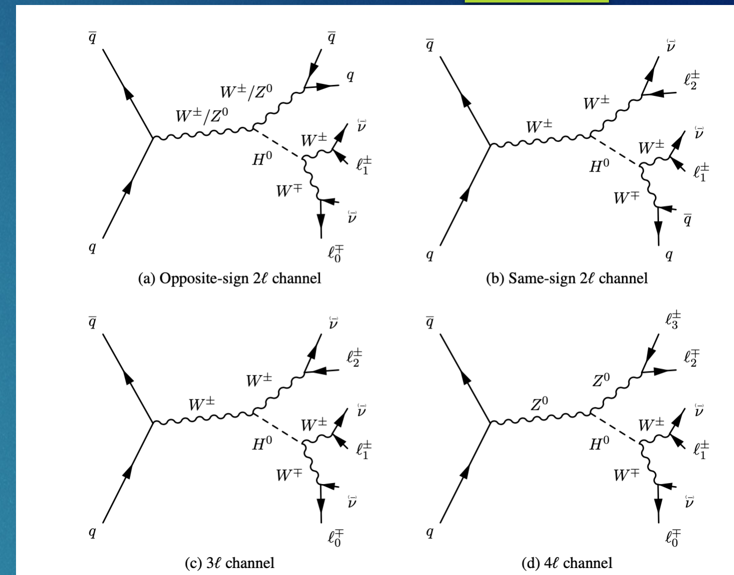

(a) Opposite-sign 2ℓ channel
(b) Same-sign 2ℓ channel
(c) 3ℓ channel
(d) 4ℓ channel

- subdivision into several SRs
- MVA discriminants to maximise the sensitivity in each channel

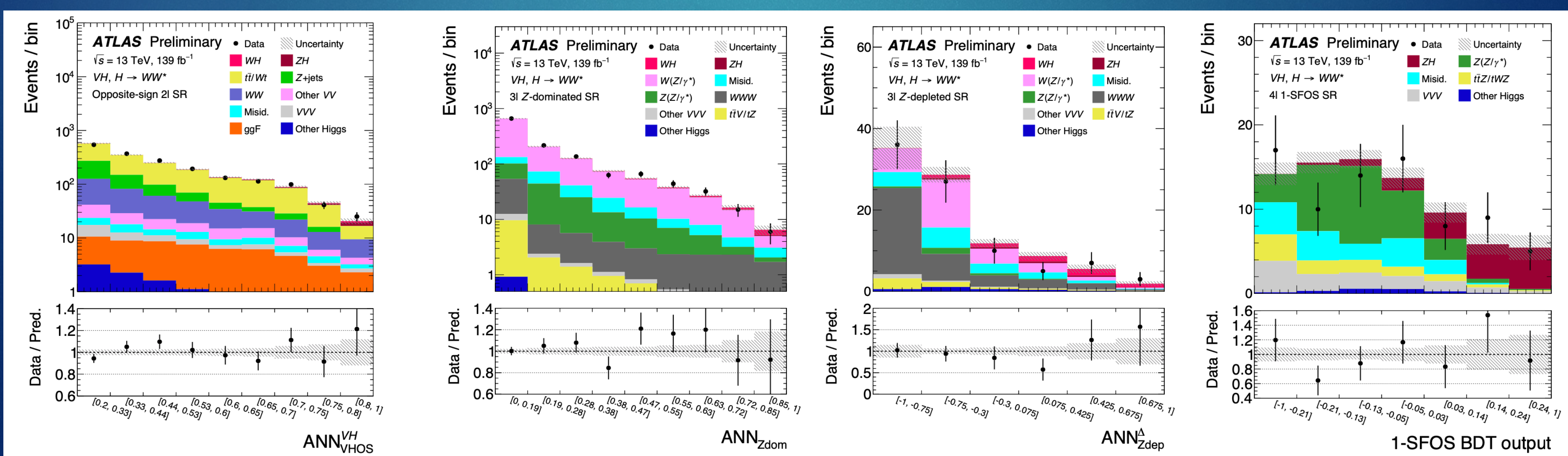

VH, H→WW

ATLAS-CONF-2022-067

- observed combined significance : 4.6σ
- Statistical uncertainties dominating
- WH and ZH measurements compatible at level of 2.1σ
- STXS results in finalization phase

$$\mu_{VH} = 0.92^{+0.21}_{-0.20}(\text{stat.})^{+0.14}_{-0.12}(\text{syst.})\,,$$

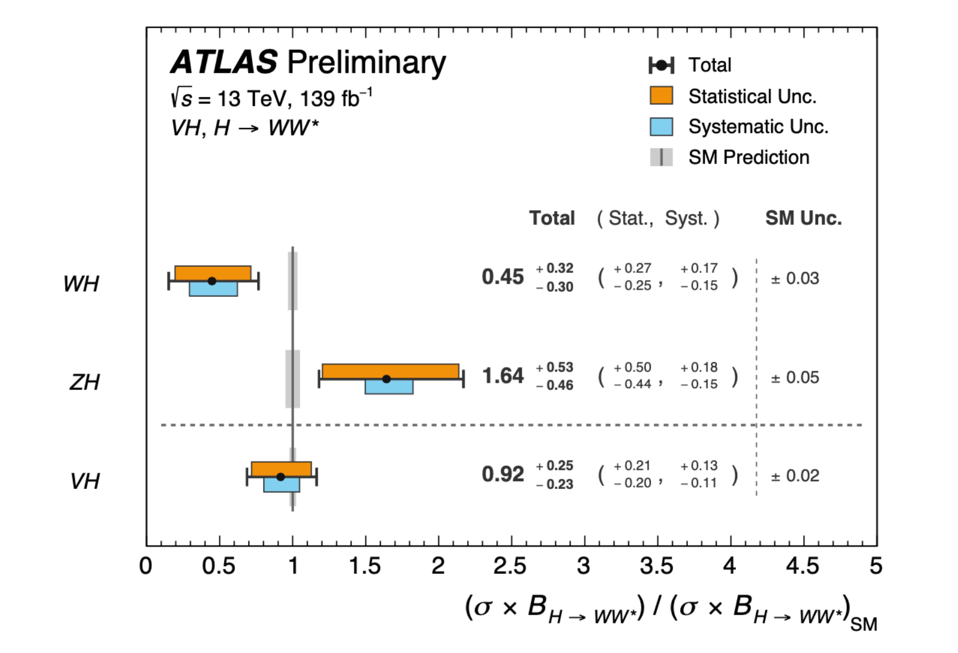

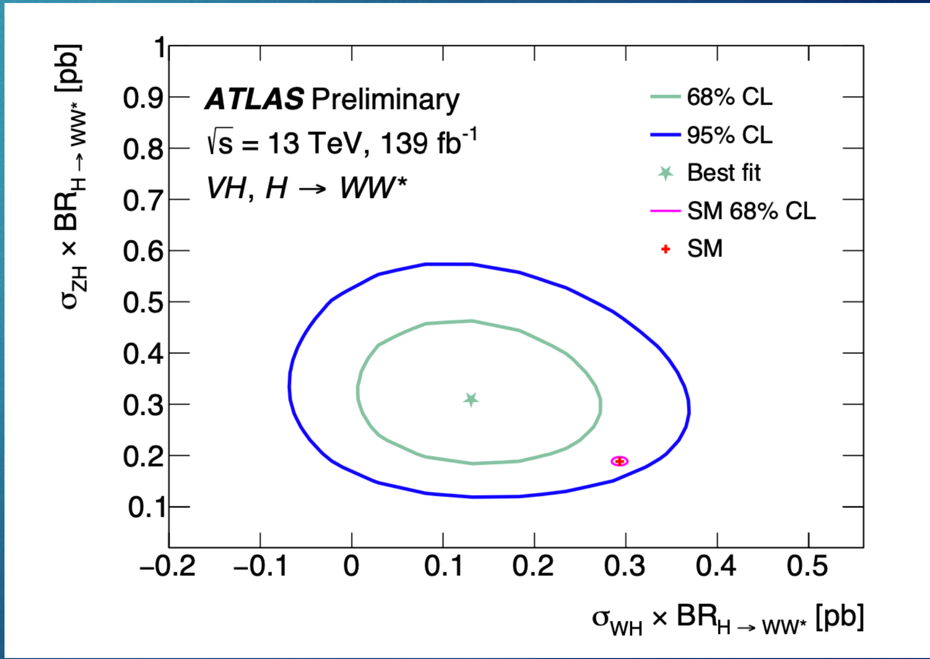

Conclusions

- Analyses of LHC Run2 data led to a large improvement on the couplings measurement precision

- All results compatible with the SM expectations so far

- Run3 has just started at 13.6 TeV, already ~30/fb collected

→ great potential to improve precision and to probe BSM with more then 2x Higgs Bosons collected

ATLAS-CONF-2023-003

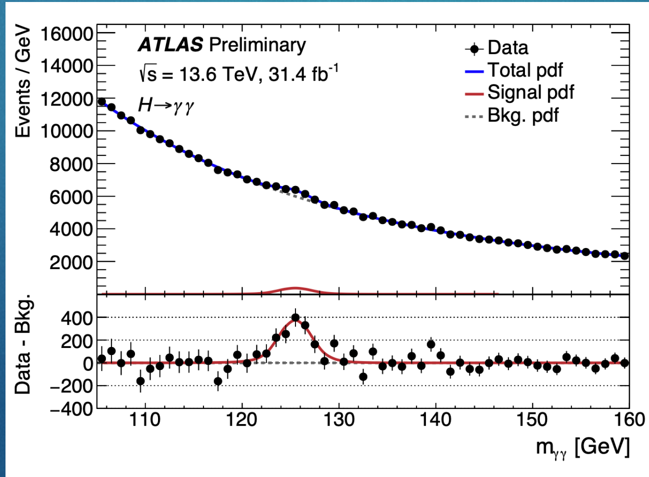

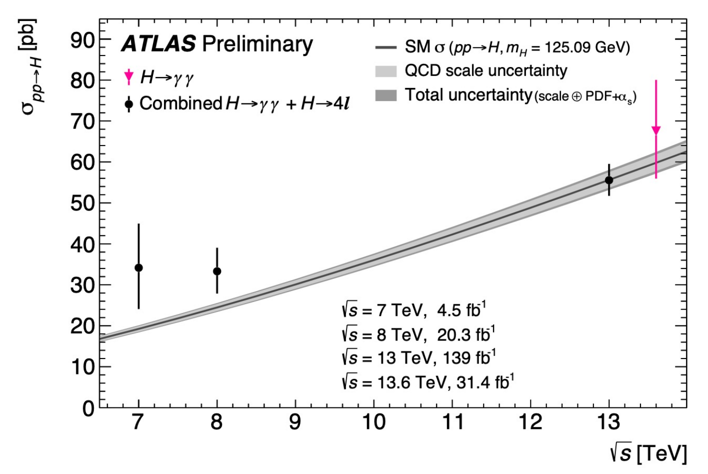

Backup

Methods - Simplified Template Cross Sections (STXS)

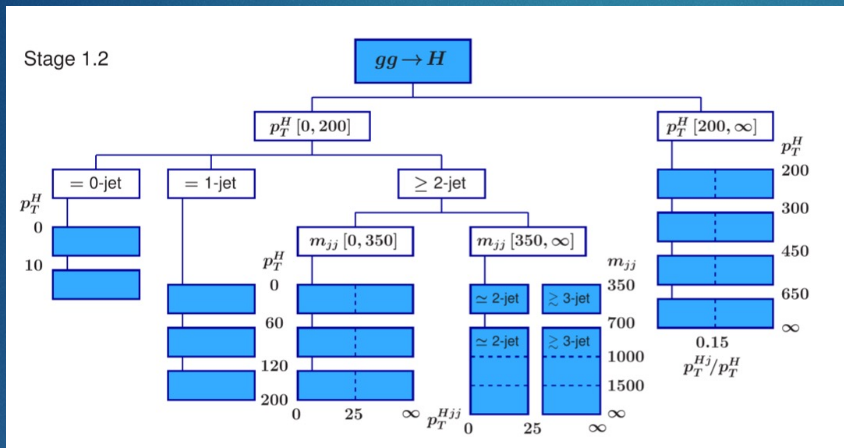

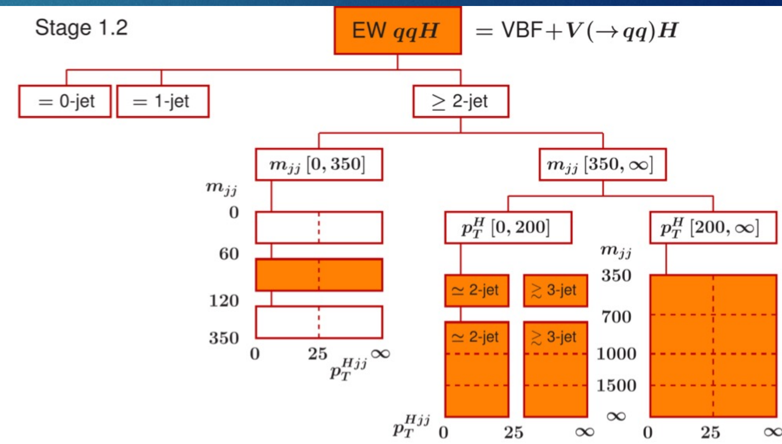

- split production phase space in multiple regions (bins) and measure the cross-section in each
  - designed to optimize the signal and BSM sensitivity
  - minimize theoretical uncertainties
- Bin split based on number of jets, p_T^H, m_{jj}, p_T^V on truth level
- Bins can be chosen/merged depending on each channel's statistics

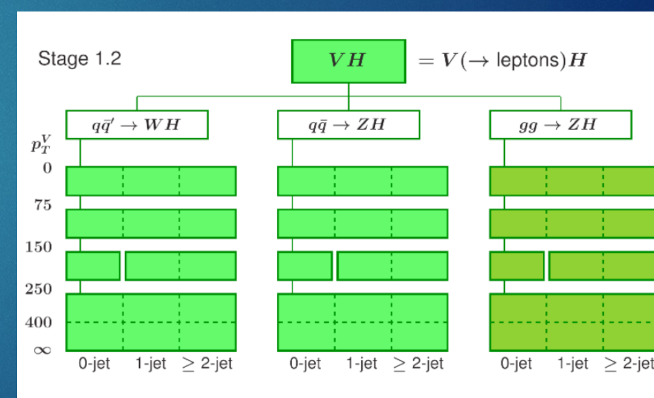

CERN-EP-2022-078
ATLAS-CONF-2022-067

H→WW

- ggF, VBF and VH production analysed
- large H->WW BR allows sensitivity to stat-limited production modes (VBF, VH)
- angle between the two charged leptons from Higgs small
  - due to the spin-0 of the Higgs boson and the chiral structure of the weak decays
  - separate the signal from the main backgrounds
- CR to check/normalize main background
  - mis-identified leptons from full

    data-driven estimation

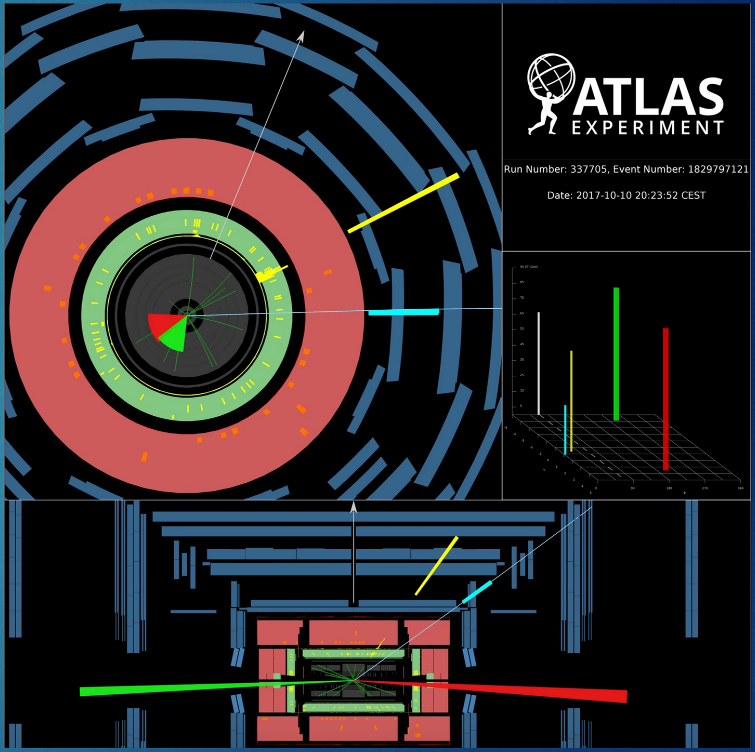

CERN-EP-2022-094

H→$\gamma\gamma$ systematic uncertainties

Table 7: Expected contributions from the main sources of systematic uncertainty to the total uncertainty in the measurement of the cross-section times $H \to \gamma\gamma$ branching ratio for each of of the main Higgs boson production processes. The uncertainty from each source ($\Delta\sigma$) is shown as a fraction of the total expected cross-section (σ).

	ggF + $b\bar{b}$H	VBF	WH	ZH	$t\bar{t}H$	tH
Uncertainty source	$\Delta\sigma$[%]	$\Delta\sigma$[%]	$\Delta\sigma$[%]	$\Delta\sigma$[%]	$\Delta\sigma$[%]	$\Delta\sigma$[%]
Theory uncertainties						
Higher-order QCD terms	±1.4	±4.1	±4.1	±12	±2.8	±16
Underlying event and parton shower	±2.5	±16	±2.5	±4.0	±3.6	±48
PDF and α_s	< ±1	±2.0	±1.4	±2.3	< ±1	±5.8
Matrix element	< ±1	±3.2	< ±1	±1.2	±2.5	±8.2
Heavy-flavour jet modelling in non-$t\bar{t}H$ processes	< ±1	< ±1	< ±1	< ±1	< ±1	±13
Experimental uncertainties						
Photon energy resolution	±3.0	±3.0	±3.8	±4.8	±3.0	±12
Photon efficiency	±2.7	±2.7	±3.3	±3.6	±2.9	±9.3
Luminosity	±1.8	±2.0	±2.4	±2.7	±2.2	±6.6
Pile-up	±1.4	±2.2	±2.0	±2.3	±1.4	±7.3
Background modelling	±2.0	±4.6	±3.6	±7.2	±2.5	±63
Photon energy scale	< ±1	< ±1	< ±1	±1.3	< ±1	±5.6
Jet/E_T^{miss}	< ±1	±6.8	< ±1	±2.2	±3.5	±22
Flavour tagging	< ±1	< ±1	< ±1	< ±1	±1.5	±3.4
Leptons	< ±1	< ±1	< ±1	< ±1	< ±1	±1.8
Higgs boson mass	< ±1	< ±1	< ±1	< ±1	< ±1	< ±1

Table 8: Summary of the leading sources of systematic uncertainty in the measurement of the Higgs boson signal strength.

Uncertainty source	$\Delta\mu$ [%]
Theory uncertainties	
Higher-Order QCD Terms	±3.8
Branching Ratio	±3.0
Underlying Event and Parton Shower	±2.5
PDF and α_s	±2.1
Matrix Element	±1.0
Modeling of Heavy Flavor Jets in non-$t\bar{t}H$ Processes	< ±1
Experimental uncertainties	
Photon energy resolution	±2.8
Photon efficiency	±2.6
Luminosity	±1.8
Pile-up	±1.5
Background modelling	±1.3
Photon energy scale	< ±1
Jet/E_T^{miss}	< ±1
Flavour tagging	< ±1
Leptons	< ±1
Higgs boson mass	< ±1

CERN-EP-2022-094

H→γγ

EVs components along the c_k SMEFT parameter

ATLAS $\sqrt{s}$=13 TeV 139fb^{-1}; H→γγ

	c_{HG}	c_{uG}	c_{uH}	c_{HW}	c_{HB}	c_{HWB}	c_{W}	c_{uW}	c_{uB}	$c_{Hl}^{(3)}$	c_{ll}'	c_{HDD}	c_{Hbox}	$c_{Hq}^{(3)}$	c_{Hu}	c_{Hd}	$c_{Hq}^{(1)}$
EV12	-0.00	-0.01	-0.15	0.01	-0.20	-0.36	-0.00	0.02	-0.01	-0.13	-0.16	-0.06	0.00	-0.00	0.37	-0.30	0.69
EV11	0.00	-0.01	0.04	0.01	-0.03	-0.05	-0.00	-0.02	0.00	-0.10	0.03	-0.00	0.00	0.00	0.06	-0.05	0.11
EV10	-0.00	-0.00	0.06	0.02	-0.09	-0.13	-0.00	0.37	-0.00	0.05	-0.02	-0.00	0.00	-0.00	0.01	0.02	-0.14
EV9	-0.00	0.01	0.03	0.09	-0.38	-0.65	-0.00	-0.08	-0.01	-0.17	0.03	-0.08	0.00	-0.02	0.13	0.04	-0.56
EV8	-0.00	0.27	0.38	0.02	0.06	0.10	0.00	0.02	0.00	-0.78	0.37	0.07	-0.00	0.01	-0.04	0.00	0.09
EV7	-0.00	0.03	0.03	0.09	0.15	0.32	0.00	0.00	0.00	0.02	0.01	0.05	0.00	-0.10	0.83	-0.25	-0.31
EV6	0.01	-0.24	0.01	-0.90	0.21	-0.14	0.01	0.01	0.01	-0.11	0.01	0.01	-0.00	0.15	0.10	-0.03	-0.08
EV5	-0.02	0.64	-0.09	-0.24	0.04	-0.06	0.00	0.00	0.00	0.15	-0.09	-0.01	-0.00	0.05	0.02	-0.01	-0.02
EV4	-0.01	0.68	-0.06	-0.08	0.01	-0.04	0.00	-0.01	-0.00	0.13	-0.07	-0.01	0.00	0.08	0.00	-0.00	-0.01
EV3	-0.01	0.05	-0.01	-0.17	0.03	-0.04	0.00	0.00	0.00	-0.01	-0.01	0.00	-0.00	-0.98	-0.07	0.02	0.03
EV2	-0.85	-0.02	0.00	-0.14	-0.44	0.25	-0.01	-0.01	-0.02	-0.01	0.00	-0.00	0.00	0.01	0.00	-0.00	-0.00
EV1	-0.53	-0.02	0.00	0.23	0.71	-0.40	0.02	0.02	0.04	0.01	-0.00	0.00	-0.00	-0.00	-0.00	0.00	0.00

	c_{He}	$c_{Hl}^{(1)}$	c_{G}	$c_{qq}^{(1)}$	$c_{qq}^{(1)'}$	$c_{qq}^{(3)}$	$c_{qq}^{(3)'}$	c_{uu}	c_{uu}'	$c_{ud}^{(8)}$	$c_{qu}^{(1)}$	$c_{qu}^{(8)}$	$c_{qd}^{(8)}$	$c_{ud}^{(1)}$	c_{eH}	c_{dH}	
EV12	0.10	0.14	0.14	0.00	-0.02	-0.05	-0.01	0.00	-0.02	0.00	0.00	-0.01	-0.00	-0.00	0.00	0.00	λ =0.0067
EV11	0.01	0.02	-0.95	-0.00	0.15	0.05	0.11	-0.01	0.13	-0.01	-0.01	0.09	-0.00	0.00	-0.00	0.00	λ =0.0108
EV10	0.02	0.03	-0.05	0.00	0.04	-0.89	0.06	0.00	0.03	0.00	-0.00	0.02	0.00	0.00	0.00	0.00	λ =0.027
EV9	0.09	0.12	0.02	-0.00	-0.01	0.18	-0.02	-0.00	-0.01	-0.00	-0.00	-0.01	-0.00	-0.00	-0.00	0.00	λ =0.038
EV8	0.00	0.00	0.09	-0.00	-0.03	-0.06	-0.04	0.00	-0.03	0.00	0.00	-0.02	-0.00	-0.00	-0.00	-0.00	λ =0.075
EV7	-0.04	-0.05	0.00	0.00	0.00	-0.01	0.00	0.00	0.00	-0.00	0.00	0.00	-0.00	-0.00	-0.00	0.00	λ =0.89
EV6	0.00	0.01	0.03	0.00	0.05	0.00	0.08	0.00	0.05	0.00	0.00	0.03	0.00	-0.00	-0.00	-0.00	λ =1.78
EV5	0.00	0.00	-0.19	-0.02	-0.28	-0.04	-0.52	-0.01	-0.27	-0.03	-0.01	-0.16	-0.03	0.00	-0.00	-0.00	λ =2.87
EV4	0.00	0.00	0.14	0.01	0.27	0.06	0.56	0.02	0.26	0.04	0.01	0.17	0.04	-0.00	-0.00	0.00	λ =20.2
EV3	0.00	0.00	0.01	0.00	0.01	0.00	0.03	0.00	0.01	0.00	0.00	0.01	0.00	-0.00	0.00	-0.00	λ =106
EV2	-0.00	-0.00	0.00	0.00	0.00	0.00	0.01	0.00	0.00	0.00	0.00	0.00	0.00	-0.00	0.00	0.00	λ =34473
EV1	-0.00	-0.00	-0.00	0.00	-0.00	-0.00	-0.00	0.00	-0.00	-0.00	0.00	-0.00	-0.00	-0.00	-0.00	-0.00	λ =346827

Eur. Phys. J. C 80 (2020) 957

H→ZZ systematic uncertainties

Table 6 The impact of the dominant systematic uncertainties (in percent) on the cross-sections in production bins of the Production Mode Stage and the Reduced Stage 1.1. Similar sources of systematic uncertainties are grouped together: luminosity (Lumi.), electron/muon reconstruction and identification efficiencies and pile-up modelling (e, μ, pile-up), jet energy scale/resolution and b-tagging efficiencies (Jets, flav. tag), uncertainties in reducible background (reducible bkg), theoretical uncertainties in ZZ^* background and tXX background, and theoretical uncertainties in the signal due to parton distribution function (PDF), QCD scale (QCD) and parton showering algorithm (Shower). The uncertainties are rounded to the nearest 0.5%, except for the luminosity uncertainty, which is measured to be 1.7% and increases for the VH signal processes due to the simulation-based normalisation of the VVV background

Measurement	Experimental uncertainties [%]				Theory uncertainties [%]				
					Background		Signal		
	Lumi.	e, μ, pile-up	Jets, flav. tag	Reducible bkg	ZZ^*	tXX	PDF	QCD	Shower
Inclusive cross-section									
	1.7	2.5	0.5	< 0.5	1	< 0.5	< 0.5	1	2
Production mode cross-sections									
ggF	1.7	2.5	1	< 0.5	1.5	< 0.5	0.5	1	2
VBF	1.7	2	4	< 0.5	1.5	< 0.5	1	5	7
VH	1.9	2	4	1	6	< 0.5	2	13.5	7.5
ttH	1.7	2	6	< 0.5	1	0.5	0.5	12.5	4
Reduced Stage-1.1 production bin cross-sections									
gg2H-0j-p_T^H-Low	1.7	3	1.5	0.5	6.5	< 0.5	< 0.5	1	1.5
gg2H-0j-p_T^H-High	1.7	3	5	< 0.5	3	< 0.5	< 0.5	0.5	5.5
gg2H-1j-p_T^H-Low	1.7	2.5	12	0.5	7	< 0.5	< 0.5	1	6
gg2H-1j-p_T^H-Med	1.7	3	7.5	< 0.5	1	< 0.5	< 0.5	1.5	5.5
gg2H-1j-p_T^H-High	1.7	3	11	0.5	2	< 0.5	< 0.5	2	7.5
gg2H-2j	1.7	2.5	16.5	1	12.5	0.5	< 0.5	2.5	10.5
gg2H-p_T^H-High	1.7	1.5	3	0.5	3.5	< 0.5	< 0.5	2	3.5
qq2Hqq-VH	1.8	4	17	1	4	1	0.5	5.5	8
qq2Hqq-VBF	1.7	2	3.5	< 0.5	5	< 0.5	< 0.5	6	10.5
qq2Hqq-BSM	1.7	2	4	< 0.5	2.5	< 0.5	< 0.5	3	8
VH-Lep	1.8	2.5	2	1	2	0.5	< 0.5	1.5	3
ttH	1.7	2.5	5	0.5	1	0.5	< 0.5	11	3

CERN-EP-2022-078
ATLAS-CONF-2022-067

H→WW systematic uncertainties

Table 6: Breakdown of the main contributions to the total uncertainty in $\sigma_{\mathrm{ggF+VBF}} \cdot \mathcal{B}_{H\to WW^*}$, $\sigma_{\mathrm{ggF}} \cdot \mathcal{B}_{H\to WW^*}$, and $\sigma_{\mathrm{VBF}} \cdot \mathcal{B}_{H\to WW^*}$, relative to the measured value. The individual sources of systematic uncertainties are grouped together. The sum in quadrature of the individual components differs from the total uncertainty due to correlations between the components.

Source	$\frac{\Delta\sigma_{\mathrm{ggF+VBF}}\cdot\mathcal{B}_{H\to WW^*}}{\sigma_{\mathrm{ggF+VBF}}\cdot\mathcal{B}_{H\to WW^*}}$ [%]	$\frac{\Delta\sigma_{\mathrm{ggF}}\cdot\mathcal{B}_{H\to WW^*}}{\sigma_{\mathrm{ggF}}\cdot\mathcal{B}_{H\to WW^*}}$ [%]	$\frac{\Delta\sigma_{\mathrm{VBF}}\cdot\mathcal{B}_{H\to WW^*}}{\sigma_{\mathrm{VBF}}\cdot\mathcal{B}_{H\to WW^*}}$ [%]
Data statistical uncertainties	4.6	5.1	15
Total systematic uncertainties	9.5	11	18
MC statistical uncertainties	3.0	3.8	4.9
Experimental uncertainties	5.2	6.3	6.7
Flavor tagging	2.3	2.7	1.0
Jet energy scale	0.9	1.1	3.7
Jet energy resolution	2.0	2.4	2.1
$E_{\mathrm{T}}^{\mathrm{miss}}$	0.7	2.2	4.9
Muons	1.8	2.1	0.8
Electrons	1.3	1.6	0.4
Fake factors	2.1	2.4	0.8
Pileup	2.4	2.5	1.3
Luminosity	2.1	2.0	2.2
Theoretical uncertainties	6.8	7.8	16
ggF	3.8	4.3	4.6
VBF	3.2	0.7	12
WW	3.5	4.2	5.5
Top	2.9	3.8	6.4
$Z\tau\tau$	1.8	2.3	1.0
Other VV	2.3	2.9	1.5
Other Higgs	0.9	0.4	0.4
Background normalizations	3.6	4.5	4.9
WW	2.2	2.8	0.6
Top	1.9	2.3	3.4
$Z\tau\tau$	2.7	3.1	3.4
Total	10	12	23

Table 11: Breakdown of the average contributions to the total uncertainties in percentage on the observed values of the signal strengths for the combined 1-POI ($\sigma_{VH} \times \mathcal{B}_{H\to WW^*}$) and 2-POI ($\sigma_{WH} \times \mathcal{B}_{H\to WW^*}$ and $\sigma_{ZH} \times \mathcal{B}_{H\to WW^*}$) fits. Indentation is used to denote subcategories. "Floating normalisation" refers to the uncertainties on the normalisation factors obtained using control regions. The quadrature sum of the individual sources may differ from the total uncertainty due to correlations.

Source	$\frac{\Delta(\sigma_{VH}\times\mathcal{B}_{H\to WW^*})}{\sigma_{VH}\times\mathcal{B}_{H\to WW^*}}$ [%]	$\frac{\Delta(\sigma_{WH}\times\mathcal{B}_{H\to WW^*})}{\sigma_{WH}\times\mathcal{B}_{H\to WW^*}}$ [%]	$\frac{\Delta(\sigma_{ZH}\times\mathcal{B}_{H\to WW^*})}{\sigma_{ZH}\times\mathcal{B}_{H\to WW^*}}$ [%]
Statistical uncertainties in data	22.3	57.9	28.4
Systematic uncertainties	13.3	36.6	9.9
Statistical uncertainties in simulation	6.4	14.4	5.9
Experimental systematic uncertainties	5.2	9.8	6.0
Electrons	1.2	1.8	1.6
Muons	2.5	2.8	4.1
Jet energy scale	0.7	2.3	0.5
Jet energy resolution	0.6	2.8	0.6
Flavour tagging	0.9	1.4	0.8
Missing transverse momentum	0.6	0.4	0.9
Pile-up	1.1	1.5	0.8
Luminosity	2.3	2.4	2.1
Mis-identified leptons	2.9	7.1	2.7
Charge-flip electrons	1.5	4.5	0.1
Theoretical uncertainties	6.0	18.6	4.7
WH	2.3	2.8	0.1
ZH	0.7	0.7	3.4
WW	1.0	3.3	0.3
$W(Z/\gamma^*)$ 0-jet	3.2	11.3	0.3
$W(Z/\gamma^*)$ ≥1-jets	0.2	0.8	0.4
$Z(Z/\gamma^*)$	0.8	1.5	0.6
VVV	2.4	12.7	0.3
Top	2.9	5.5	2.5
Z+jets	1.8	3.4	1.5
RNN shape uncertainty for $W(Z/\gamma^*)$	8.8	27.3	0.3
Floating normalisations	0.1	0.2	0.1
Total	26.0	71.0	30.1